Journal of Nuclear Materials 461 (2015) 230–235

Contents lists available at ScienceDirect

Journal of Nuclear Materials

journal homepage: www.elsevier.com/locate/jnucmat

First-principles investigation of helium dissolution and clustering at a tungsten (1 1 0) surface

Jinlong Wang, Ying Zhang, Hong-Bo Zhou, Shuo Jin, Guang-Hong Lu *

Department of Physics, Beihang University, Beijing 100191, People's Republic of China

ARTICLE INFO

Article history:
Received 28 August 2014
Accepted 10 March 2015
Available online 17 March 2015

ABSTRACT

Using a first-principles method, we have investigated dissolution, self-trapping and clustering of He at a W(1 1 0) surface. We found that the He atom is not energetically favorable at both the surface and the subsurface, but it becomes stable under the second atomic layer from the surface. The He is easier to be self-trapped to form an He cluster at the near surface in comparison with the bulk due to the larger self-trapping range and the stronger binding energy. With the formation of such He cluster, the vacancy and thus the He-vacancy complex are able to form at the near surface. The results will provide a useful reference for understanding formation of the He bubble at the W surface.

1. Introduction

Tungsten (W) and W-alloys [1–3] are considered as the most promising plasma facing materials (PFMs) because of their low sputtering erosion and good thermal properties such as high thermal conductivity and high melting temperature. However, the PFMs can be irradiated by low-energy (1–100 eV) and high flux ($\sim 10^{24}$ m^{-2} s^{-1}) hydrogen (H) isotopes and helium (He) ions, which results in retention and bubble formation of H and He. In addition, the transmutation introduced by high energy neutron irradiation also produces an appreciable concentration of H and He.

The experimental results show that the depth of trapped He is within ~25 nm and ~50 nm of the W surface if the polycrystalline W irradiated with 500 eV He ions at low temperature (300 K) [4]. The He bubbles can be clearly seen within the depth of 2 μm if the polycrystalline W irradiated with 60 eV He ions at the high temperature (2300 K) [5]. It seems that the trapping depth of He can be strongly influenced by the temperature. In a temperature range from 1000 to 2000 K, the nanostructure with an arborescent shape on the He exposure of W surface, called W fuzz, is easily formed [6,7]. The fuzz consists of a very porous W network and is mechanically unstable. When the temperature is higher than 2000 K, the fuzz disappears and a rough micrometer-sized structure with many pinholes is formed [6]. The He bubbles induce serious hardening and dramatic reduction of thermal conductivity near the surface by several orders of magnitudes [8,9], which enhances erosion under a high heat load, e.g. leading to a repeated surface exfoliation of about 1 μm thick layer [10].

Theoretically, the most stable interstitial site for He in intrinsic W is shown to be a tetrahedral interstitial site (TIS) [11,12]. He in W is mobile even below room temperature, and the experimental migration energy of He is 0.28 eV [13], while the calculated migration energy is much lower, around 0.06 eV [14]. The discrepancy between the experimental and computational results can be explained by the large binding energy that exists between He atoms [14]. The binding energies between two He atoms is calculated as 1.03 eV [14] and the self-trapping length (capture radius) of He has been assumed to be equal to the lattice parameter [15]. The strong He–He binding energy reveals that the He is easily trapped not only at lattice vacancies, impurities, and vacancy-impurity complexes, but also by other He atoms [14].

So far the theoretical work mainly focuses on the adsorption and migration of H on W surface [16,17], especially for low-Miller-index surfaces such as W(1 1 0) [18,19] and W(1 0 0) [19,20]. However, little has been done on the behaviors of He at the W surface from the first principles. With the consideration that the W(1 1 0) surface is most stable, in this work, we have investigated the dissolution and clustering of He at the W(1 1 0) surface using a first-principles method based on density functional theory (DFT). The results will provide a useful reference for understanding the formation mechanism of the He bubble as well as the fuzz at the W surface.

2. Methodology

The first-principles calculations are performed with the Vienna *Ab-Initio* Simulation Package (VASP) [21,22] based on DFT. The W-6*s*, W-5*d* and He-1*s* electrons are treated as valence electrons,

* Corresponding author.
E-mail addresses: zhyi@buaa.edu.cn (Y. Zhang), lgh@buaa.edu.cn (G.-H. Lu).

http://dx.doi.org/10.1016/j.jnucmat.2015.03.026
0022-3115/

while interaction between the ionic cores and the valence electrons is described by the projector augmented wave (PAW) potentials [23]. Electron exchange and correlation is performed within the generalized gradient approximation (GGA) using the Perdew–Wang functional [24]. The kinetic energy cutoff for the plane-wave basis set is set as 400 eV. The first-order Methfessel–Paxton method [25] is used for the Fermi surface smearing with a width of 0.1 eV. The convergence criteria for the electronic self-consistent iteration and the ionic relaxation are set as 10^{-5} eV and 0.01 eV/Å, respectively.

Brillouin zone integration is performed using Monkhorst–Pack grids [26] for all calculations. The calculated lattice constant of 3.175 Å agrees well with the experimental value of 3.16 Å. As shown in Fig. 1, the dimensions of our surface slab model of the W(1 1 0) surface is $9.53 \times 8.98 \times 31.43$ Å^3, which contain 9 atomic layers and 10 Å vacuum. The bottom layer is fixed to the bulk structure to mimic a semi-infinite crystal. The *k*-point sampling is chosen as $3 \times 3 \times 1$, which ensures enough *k*-point density.

3. Results and discussion

3.1. Formation energy of vacancy

First, we investigate the formation energy of vacancy at the W surface. The formation energy of vacancy in the bulk was calculated as 3.07 eV, consistent with 3.11 eV in the previous work [27]. As shown in Fig. 2, the formation energy of vacancy increases from 1.85 eV at the surface to 3.07 eV at the depth of the fifth layer. The results reveal that the effect of the surface can be ignored under the fourth atomic layer of the W(1 1 0) surface. Thus, we consider the dissolution of He under the fourth layer from the surface corresponds to those with the bulk condition.

3.2. Dissolution of single He atom

In order to investigate the absorption behavior of He atom on the W(1 1 0) surface, we examine the adsorption energies of all the potential sites for He, including the top site, the short-bridge site, the long-bridge site, and the hollow site. It is found that the He atom cannot be adsorbed on the W(1 1 0) surface, quite different from H. The H can be absorbed tightly on the threefold hollow site of the W(1 1 0) surface with the adsorption energy of −0.75 eV [19]. This is because He has a closed-shell electronic structure and its interaction with W is expected to be very weak, leading to the escape of He from the W surface.

Next, we investigate the dissolution behavior of a single He atom at the W(1 1 0) surface (below the first surface W layer). The He solution energy E_s at the W surface is defined as

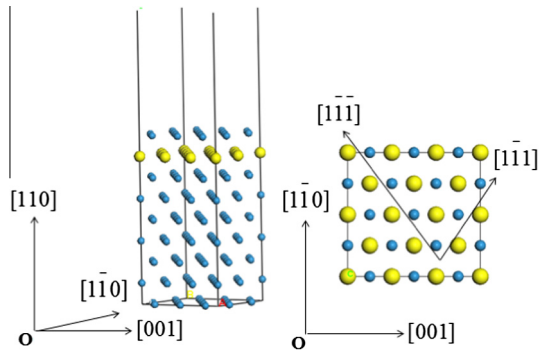

Fig. 1. The slab model of the W(1 1 0) surface. The larger yellow spheres represent the 2nd layer atoms in order to show the surface lattice points more clearly. (For interpretation of the references to color in this figure legend, the reader is referred to the web version of this article.)

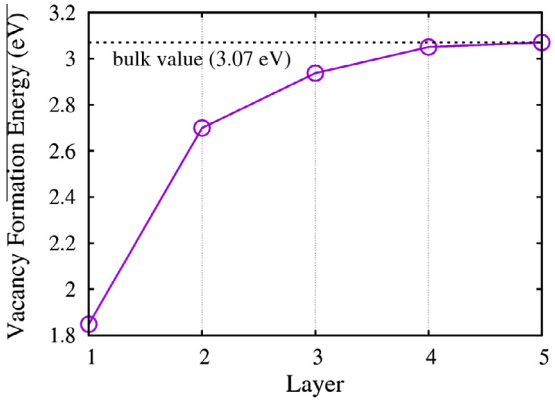

Fig. 2. The vacancy formation energy as a function of the *n*th layer from the surface. The dash line represents the vacancy formation energy in the bulk (3.07 eV).

$$E_s = E_{W,He} - E_W - E_{He}, \quad (1)$$

where $E_{W,He}$ and E_W are the total energies of the W surface slab supercell with and without He atom, respectively. E_{He} is the energy of an isolated He atom. The OIS for He is not energetically favorable site in comparison with the TIS [14,28]. As a matter of fact, the OIS for He is considered to be a saddle point during the diffusion process of TIS → OIS → TIS. The He at OIS will relax to the TIS once given a perturbation. Consequently, here we did not consider the dissolution of the He at the OIS in the paper.

As shown in Fig. 3(a), one He atom is set at different TIS's at the W(1 1 0) surface. Fig. 3(b) shows the solution energies of He as a function of depth for both the relaxed and unrelaxed cases. For the convenience of comparison, the formation energy of the TIS He in the bulk is also calculated and shown here. The formation energy of TIS He is 6.15 eV, which agrees well with the calculated value of 6.16 eV in the previous work [14]. It is found that the He escapes from the *A*, *B*, *C* sites to the vacuum after relaxation, which reveals that the He cannot stay stably at the subsurface (within the depth of ~2.8 Å). The formation energy of He at the site from "*D*" to "*L*" fluctuates around 6.1 eV (6.1 ± 0.05 eV), a little lower than that in the bulk. For the unrelaxed case, it is found that the solution energy increases with the increasing of depth before ~2 Å. After that, the solution energy decreases rapidly and converges to ~7.4 eV, ~1.3 eV higher than that of relaxed system.

3.3. He–He interaction and self-trapping

In order to understand the self-trapping of He at the W(1 1 0) surface, we further investigate the interactions between two He atoms. The binding energy between two He atoms E_b can be obtained by

$$E_b = 2E_{W,He} - E_{W,2He} - E_W, \quad (2)$$

where $E_{W,2He}$ is the energy of the supercell with two He atoms. The $E_{W,He}$ and E_W are the total energies of the W surface slab supercell with and without He atom, respectively. Here, the positive binding energy indicates attraction between two He atoms, while the negative binding energy indicates repulsion.

We put two He atoms at the TIS with the different depth from the surface (between 2nd and 3rd, 3rd and 4th, 4th and 5th layers, respectively). As shown in the inset of Fig. 4, the first He is situated at the site labeled as '*A*', and the second He is situated at the sites labeled from 1 to 8, respectively. All the calculated results are tabulated in Table 1 and shown in Fig. 4. The initial distances of the two He atoms increase gradually from case 1 to case 8, but change (mainly decrease) after relaxation.

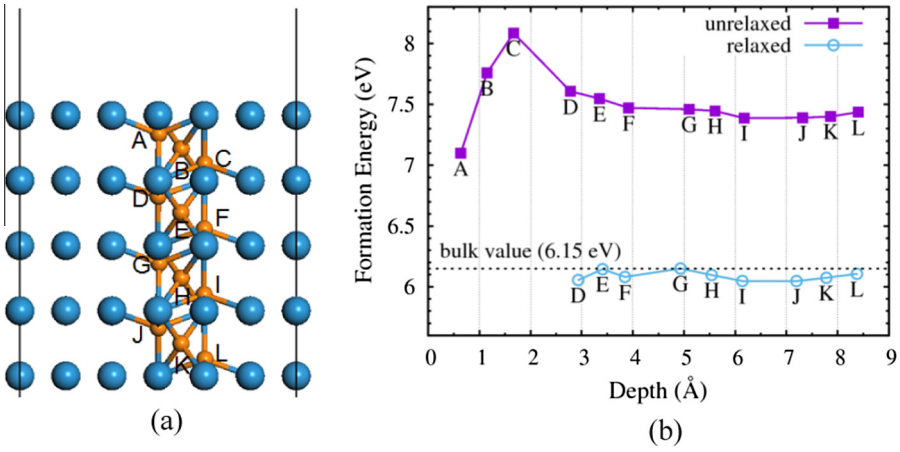

Fig. 3. (a) Dissolution sites of He at the W(1 1 0) surface, where the larger blue spheres and the smaller orange spheres represent W and He atoms, respectively. (b) Variation of the formation energy of He with different dissolution depth at the W(1 1 0) surface. The line is a guide for the eyes. (For interpretation of the references to color in this figure legend, the reader is referred to the web version of this article.)

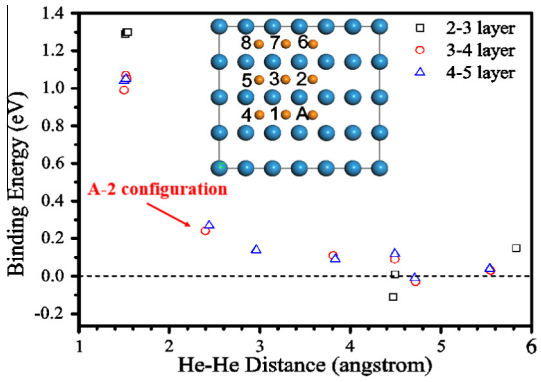

Fig. 4. Self-trapping of He at the W(1 1 0) surface. The inset labels the He–He positions before relaxation, in which the first He is situated at the site labeled as *A*, and the second He is situated at the sites labeled from 1 to 8, respectively. The figure does not contain the binding energy of He–He with *A*-5 configuration at the depth of 2–3 layer due to the formation of one vacancy.

As shown in Fig. 4, basically the two He atoms attract with each other to form the He_2 cluster within certain distance at the different surface layers. At the depth of the 2–3 layer, the two He atoms form He_2 cluster with a binding energy of ~1.3 eV and distance of ~1.5 Å after relaxation if the He–He initial distance is less than ~4 Å. At the depth of the 3–4 and 4–5 layer, the two He atoms form the He_2 cluster with the initial He–He distance less than ~3 Å except the *A*-2 configuration. The He–He distance is ~1.5 Å, similar to that at the 2–3 layer, but the binding energy is ~1.0 eV, 0.3 eV lower than that at the 2–3 layer. Beyond the trapping distance, the He–He binding energy approaches to zero.

Table 1
The initial and final distances (d_i and d_f) and binding energies (E_b) of two He atoms in different depth below the surface. The positive binding energy indicates attraction, while the negative binding energy indicates repulsion.

Position	d_i (Å)	2–3 layer		3–4 layer		4–5 layer	
		d_f (Å)	E_b (eV)	d_f (Å)	E_b (eV)	d_f (Å)	E_b (eV)
1	1.60	1.51	1.29	1.50	0.99	1.50	1.04
2	2.40	1.51	1.29	2.40	0.24	2.44	0.27
3	2.80	1.53	1.30	1.52	1.07	1.52	1.05
4	3.20	1.54	1.30	1.53	1.05	2.96	0.14
5	3.90	1.48	3.89	3.81	0.11	3.83	0.09
6	4.50	4.49	0.01	4.49	0.09	4.49	0.12
7	4.76	4.47	−0.11	4.72	−0.03	4.71	−0.01
8	5.60	5.83	0.15	5.55	0.03	5.54	0.04

For the case of the depth between 2nd and 3rd layer, the He–He distances become shorter to almost the same value of ~1.5 Å for the case of 1–5, suggesting an attractive interaction, while the He–He distances are almost unchanged for the case of 6–8, as shown in Table 1 and Fig. 5. The binding energies for the case of 1–4 are about 1.3 eV. The He–He binding energy is 1.02 eV in the bulk, consistent with previous calculated value 1.03 eV [14]. The He–He binding energies at the near surface are higher than that in the bulk, indicating that the self-trapping of He at the near surface is stronger than that at the bulk. Also, it is interesting to see the He–He cluster exhibits directionality due to the lattice anisotropy. In the case of 1–4 (Fig. 5), the He_2 clusters orientate approximately along the ⟨1 1 1⟩ crystal direction, which is different from that in the bulk. The He_2 cluster in the bulk was found to orientate along a direction close to ⟨0 1 2⟩ [29].

For the case of the site 6–8, the interaction between two He atoms is very weak due to the large He–He distances and the low binding energies (the absolutely value less than 0.15 eV). The self-trapping distance of He at the very shallow W(1 1 0) surface is about 3.9 Å according to the present calculations, which is larger than 3.17 Å in the bulk [15]. This indicates that the self-trapping of He at the surface will be more probable than in the bulk. The dissolved He atoms prefer to be self-trapped to the equilibrium He–He distance of ~1.5 Å once the He–He distance is less than 3.9 Å.

The binding energy of *A*-5 configuration at the depth of 2–3 layer is not included in Fig. 4, which is up to 3.89 eV due to the formation of He_2-vacancy complex. As shown in Fig. 5e, the He_2 cluster squeezes out one W atom to the surface from its original lattice site during the relaxation. This seems surprising, but it is inevitable to undergo such relaxation. We confirm such relaxation by removing two He atoms and making the relaxation again. It is found that the extruded W atoms move back to their original lattice sites to form the clean surface. This reveals that the formation of the He_2 cluster with the creation of a W vacancy/interstitial pair is an energetically barrierless process.

For the case of the depth between 3rd and 4th layer, the He–He distances are shortened to an almost same value of ~1.5 Å for the cases of site 1, 3 and 4. The He–He distances remain almost unchanged for the other sites. The binding energies for the case of site 1, 3 and 4 are from 0.99 eV to 1.07 eV. For the case of site 2, the binding energy is 0.24 eV despite the He–He distance remains the same as that before the relaxation. For other cases, the interaction between the two He is very weak due to the large He–He distances and the low binding energies (the absolutely value less than 0.1 eV). For the case of the depth between 4th

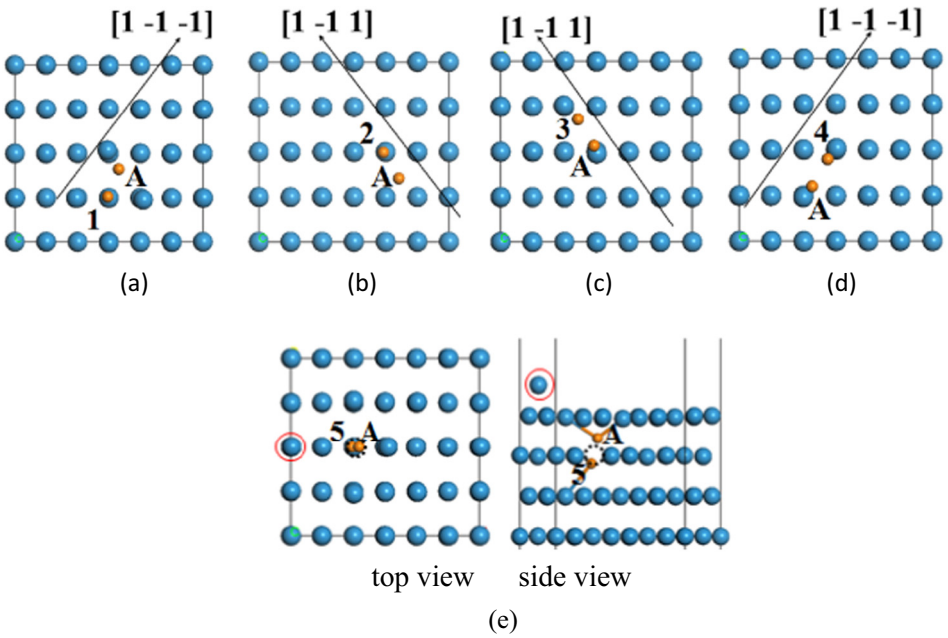

Fig. 5. The configurations for two He atoms at the depth between the 2nd and 3rd layer after relaxation. The dash circles represent the vacancy. The spheres in the red solid circles represent the W atoms that are squeezed out from the surface. (For interpretation of the references to color in this figure legend, the reader is referred to the web version of this article.)

and 5th layer, the results are similar to the case of the depth between 3rd and 4th layer, except that the cases of site 1 and 3 which is self-trapped to an equilibrium distance of ~1.5 Å with binding energies of 1.04 eV and 1.05 eV, respectively.

Now, it is clear that the final configurations can be quite different from the initial ones according to the present calculation. As mentioned in the previous study [14], the He is able to relax by as large as one lattice constant (~3 Å) so as to reduce the He–He distance. For all the configurations, the He–He distance is about 1.5 Å for the stable state of He_2 cluster. The initial configurations that decay into other configurations upon relaxation are indeed unstable. We have employed other relaxation algorithms such as the damped molecular dynamics algorithm to make further simulations, which have verified the present results.

Thus, it can be speculated that the self-trapping distance (capture radius) increases with decreasing depth from the surface, despite not all the possible occupation sites have been taken into account. This is originated from the lower vacancy formation energy at the surface, which facilitates the He self-trapping in comparison with the bulk.

Furthermore, it is very interesting to see that, at the depth of 3–4 layer and 4–5 layer, the two He atoms do not form the He_2 cluster in the *A*-2 configuration with initial He–He distance of ~2.4 Å, while they do form the He_2 cluster in the *A*-3 configuration with an larger initial distance of ~2.8 Å. Taking the case of two He at the depth of 3–4 layer as an example, the atomic configurations are shown in Fig. 6, and the variations of the displacement of *D*, *E*, *F* atoms and the He–He distances during the atomic relaxation are shown in Fig. 7a and b, respectively. In the configuration of *A*-2, the two W atoms (*D* and *E*) between two He atoms suffer rather large forces (5.91 eV/Å and 7.32 eV/Å, respectively) at the beginning of the relaxation. The force direction is along the ⟨1 1 1⟩ crystalline direction, which is the most closely packed. Along the force direction, there exists another W atom (*D*′ or *E*′) to block the movement of the W atom *D* and *E*, leading to the largest relaxation distance of only 0.29 Å (*D*) and 0.38 Å (*E*), respectively. This makes the two He atoms not aggregate finally. In contrast, in the configuration of *A*-3, only one W atom (*F*) between

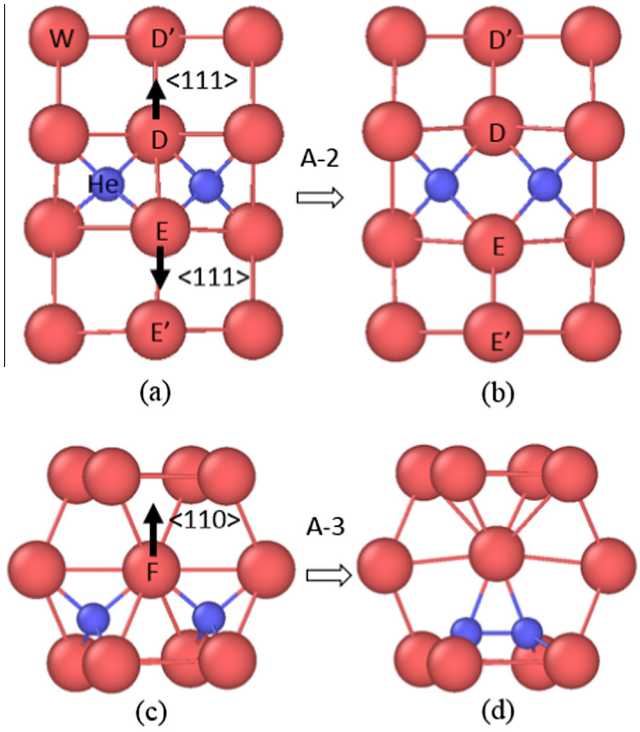

Fig. 6. The He–He configurations of *A*-2 (a) before and (b) after relaxation, and those of *A*-3 (c) before and (d) after relaxation. The smaller blue spheres represent the He atoms and the larger red spheres represent the W atoms, respectively. The shared W atoms by two He are labeled by *D*, *E* and *F*. The arrows show the force direction at the initial stage of relaxation. (For interpretation of the references to color in this figure legend, the reader is referred to the web version of this article.)

two He atoms suffers rather large force (5.0 eV/Å) at the beginning of the relaxation, and no W atoms exists along the force direction, i.e. the ⟨1 1 0⟩ crystalline direction. This leads to the largest relaxation distance of W atom (*F*) up to 0.43 Å, making the two He atoms get together finally. This is confirmed by the He–He distance

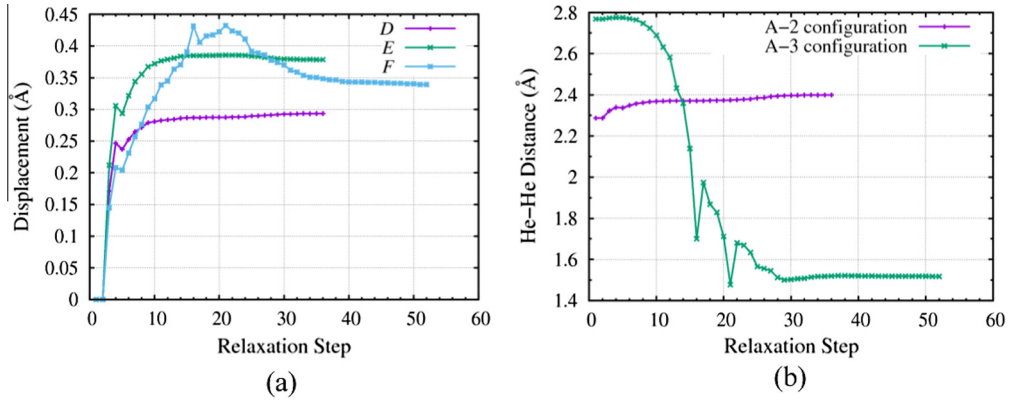

Fig. 7. (a) The variation of displacements of the W atoms of *D*, *E*, *F* (as shown in Fig. 6) and (b) the variation of the He–He distance during the relaxation.

variation during the relaxation shown in Fig. 7b. The He–He distance for the *A*-2 case never decreases to 2.2 Å, while it becomes 1.5 Å for the *A*-3 case, which satisfies the distance requirement for the He–He clustering.

3.4. He clustering

We further investigate how the He clusters with more He atoms at the W(1 1 0) surface. For the multiple dissolved He atoms, the average solution energy E_s is determined by

$$E_s = [E_{W,nHe} - E_W - nE_{He}]/n, \quad (3)$$

where n is number of He atoms.

As shown in Fig. 8(a), the He atoms are added at the surface one by one at the position labeled from 1 to 5. Only the cases of the depth between 4th and 5th layer and between 2nd and 3rd layer are shown here. It should be noted that the 5 sites are selected in order to dissolve He as much as possible with the precondition that the dissolved He will not be self-trapped with each other. The He atoms do not self-trap with other He until the addition of the 4th He atom, while they aggregate to form He_5 cluster when the 5th He is added in. The He_5 cluster approximates along the ⟨1 1 1⟩ direction again as shown in Fig. 8(a). The relaxation behaviors are different for the different depth. At the depth between 4th and 5th layer, the W atoms around He_5 cluster relax a lot and the largest displacement is up to ~0.9 Å. At the shallow location from the surface (between 2nd and 3rd layer), three W atoms around He_5 cluster are squeezed out from their lattice points with the formation of three vacancies. As a result, the He_5V_3 complex forms. As shown in Fig. 8(b), the average dissolution energy decreases slowly with the increasing number of He atoms, and exhibit a sudden decrease with the formation of He_5 cluster, which reveals the aggregation of He is energetically favorable. Here, we show the vacancies can be created by He_n cluster at the near surface. In Ni, the formation of the He_5 and He_8 clusters have been shown to originate the creation of one and two vacancy-interstitial pairs (i.e., Frenkel pair), respectively [30].

Upon the current work, the dissolved He can aggregate within the trapping distance. In addition, it is found that the He_2 and He_5 cluster can create vacancies more easily at the shallow surface than in the bulk during the relaxation. The small He clusters (or He_nV complex) may be considered to be the initial stage of He bubbles or pin hole at the surface. Some W atoms are squeezed out from the lattice site and extrude to the surface, which may be considered to be some clues for the fuzz formation. Our calculation thus will provide a useful reference for understanding of He bubble and fuzz formation, and further investigations are needed.

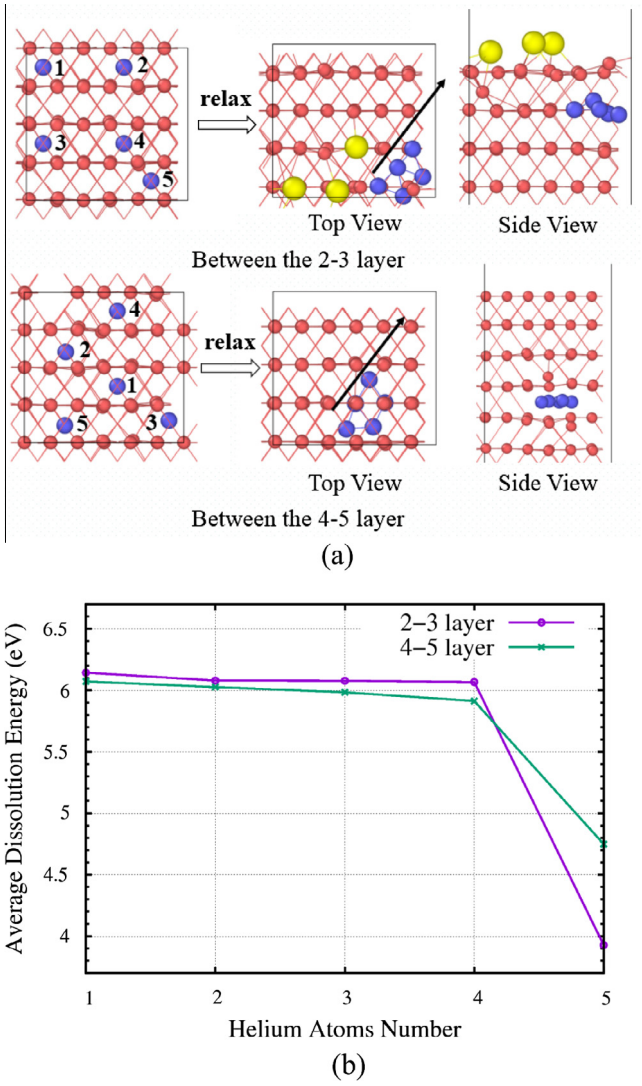

Fig. 8. (a) The He atoms (larger blue spheres) are added one by one at the sites labeled from 1 to 5 at the near surface, and the three bigger yellow spheres represent W atoms that squeeze out from the surface. (b) The variation of average dissolution energy as a function of number of He atoms. (For interpretation of the references to color in this figure legend, the reader is referred to the web version of this article.)

Finally, we note here that the surface effect for He is among several atomic layers of W surface. For example, the dissolution behavior of He does not exhibit distinct difference than that in

the bulk beyond the 4th atomic layer. Consequently, to investigate the surface effects on the dissolution and clustering of He at the W surface, the present model of first few layers of the W(1 1 0) surface is thus sufficient. On the other hand, the diffusion of He is very rapidly. So the dissolution depth of He and thus He bubble can range from tens of nanometers to microns according to the different conditions of experiments such as temperature and incident energy. We may consider that the surface effect for the He dissolution and clustering at the first few layers of W surface should play an important role on the experimentally observed He bubble as well as fuzz formation.

4. Conclusions

The dissolution and the clustering of He at the W(1 1 0) surface have been investigated by a first-principles method based on the density functional theory. The vacancy formation energy is 1.85 eV at the surface, and converges to the 3.07 eV at the depth of the fifth atomic layer that is equivalent with that at the bulk. The He atom is shown to be not energetically favorable to stay at the surface and the subsurface, but it can stay stably under the 2nd atomic layer from the surface. The formation energy of He fluctuates around 6.1 eV, but almost the same as that at the bulk (6.15 eV). The He is easier to be self-trapped to form an He cluster at the near surface in comparison with the bulk due to the larger self-trapping range and the stronger binding energy, and prefers to cluster along the ⟨1 1 1⟩ crystalline direction. The vacancies can be created with the formation of such He cluster at the surface. The results can be expected to provide a useful reference for understanding the formation of the He bubble as well as the fuzz at the W surface.

Acknowledgements

This work is supported by the National Magnetic Confinement Fusion Program with Grant No. 2013GB109002 and the National Natural Science Foundation of China with Grant No. 11405006. G.H. Lu acknowledges support from the National Natural Science Foundation of China for Distinguished Young Scientists through Grant No. 51325103.

References

[1] Z. Yang, Y.M. Yang, G.H. Lu, G.N. Luo, J. Nucl. Mater. 390–391 (2009) 136–139.
[2] L. Yue-Lin, J. Shuo, Z. Ying, Chin. Phys. B 21 (2012) 016105.
[3] X.-C. Li, X. Shu, Y.-N. Liu, F. Gao, G.-H. Lu, J. Nucl. Mater. 408 (2011) 12–17.
[4] H.T. Lee, A.A. Haasz, J.W. Davis, R.G. Macaulay-Newcombe, J. Nucl. Mater. 360 (2007) 196–207.
[5] D. Nishijima, M.Y. Ye, N. Ohno, S. Takamura, J. Nucl. Mater. 313–316 (2003) 97–101.
[6] K. Shin, S. Wataru, O. Noriyasu, Y. Naoaki, S. Tsubasa, Nucl. Fusion 49 (2009) 095005.
[7] K. Shin et al., Nucl. Fusion 49 (2009) 095005.
[8] K. Shin, T. Shuichi, O. Noriyasu, N. Dai, I. Hirotomo, Y. Naoaki, Nucl. Fusion 47 (2007) 1358.
[9] K. Shin et al., Nucl. Fusion 47 (2007) 1358.
[10] N. Yoshida, H. Iwakiri, K. Tokunaga, T. Baba, J. Nucl. Mater. 337–339 (2005) 946–950.
[11] T. Seletskaia, Y. Osetsky, R.E. Stoller, G.M. Stocks, Phys. Rev. Lett. 94 (2005) 046403.
[12] T. Seletskaia, Y. Osetsky, R.E. Stoller, G.M. Stocks, Phys. Rev. B 78 (2008) 134103.
[13] J. Amano, D.N. Seidman, J. Appl. Phys. 56 (1984) 983–992.
[14] C.S. Becquart, C. Domain, Phys. Rev. Lett. 97 (2006) 196402.
[15] K.O.E. Henriksson, K. Nordlund, A. Krasheninnikov, J. Keinonen, Appl. Phys. Lett. 87 (2005) 163113.
[16] G.-H. Lu, H.-B. Zhou, C.S. Becquart, Nucl. Fusion 54 (2014) 086001.
[17] L. Guang-Hong, Z. Hong-Bo, S.B. Charlotte, Nucl. Fusion 54 (2014) 086001.
[18] A. Nojima, K. Yamashita, Surf. Sci. 601 (2007) 3003–3011.
[19] D.F. Johnson, E.A. Carter, J. Mater. Res. 25 (2010) 315–327.
[20] K. Heinola, T. Ahlgren, Phys. Rev. B 81 (2010) 073409.
[21] G. Kresse, J. Hafner, Phys. Rev. B 47 (1993) 558–561.
[22] G. Kresse, J. Furthmüller, Comput. Mater. Sci. 6 (1996) 15–50.
[23] G. Kresse, D. Joubert, Phys. Rev. B 59 (1999) 1758.
[24] J.P. Perdew, K. Burke, M. Ernzerhof, Phys. Rev. Lett. 77 (1996) 3865.
[25] M. Methfessel, A.T. Paxton, Phys. Rev. B 40 (1989) 3616.
[26] H.J. Monkhorst, J.D. Pack, Phys. Rev. B 13 (1976) 5188.
[27] C.S. Becquart, C. Domain, Nucl. Instrum. Methods B 255 (2007) 23–26.
[28] H.-B. Zhou, Y.-L. Liu, S. Jin, Y. Zhang, G.N. Luo, G.-H. Lu, Nucl. Fusion 50 (2010) 115010.
[29] C.S. Becquart, C. Domain, J. Nucl. Mater. 386–388 (2009) 109–111.
[30] T. Tomoyuki, K. Ryo, O. Shuji, M.I. Atsushi, Model. Simul. Mater. Sci. 22 (2014) 015002.